

M ethanol-water solutions: a bi-percolating liquid mixture

L. Dougan⁽¹⁾, S. P. Bates⁽¹⁾, R. Hargreaves⁽¹⁾, J. P. Fox⁽¹⁾,
J. Crain^{(1) (2)}, J. L. Finney⁽³⁾, V. Reat⁽⁴⁾, and A. K. Soper⁽⁵⁾⁽¹⁾ School of Physics, The University of Edinburgh, Mayfield Road, Edinburgh EH9 3JZ, UK⁽²⁾ IBM T. J. Watson Research Center, 1101 Kitchawan Road, Yorktown Heights, New York, 10598, USA⁽³⁾ Department of Physics and Astronomy, University College London, Gower Street, London, WC1E 6BT, UK⁽⁴⁾ Institut de Pharmacie et de Biologie Structurale, UMR 5089 - CNRS/UPS,
Laboratoire "RMN et interactions protéines-membranes",
205 Route de Narbonne, 31077 Toulouse Cedex, FRANCE. and⁽⁵⁾ ISIS Facility, Rutherford Appleton Laboratory, Chilton, Didcot, Oxon, OX11 0QX, UK
(Dated: April 14, 2024)

An extensive series of neutron diffraction experiments and molecular dynamics simulations has shown that mixtures of methanol and water exhibit extended structures in solution despite the components being fully miscible in all proportions. Of particular interest is a concentration region (methanol mole fraction between 0.27 and 0.54) where both methanol and water appear to form separate, percolating networks. This is the concentration range where many transport properties and thermodynamic excess functions reach extremal values. The observed concentration dependence of several of these material properties of the solution may therefore have a structural origin.

PACS numbers: 82.70.Jv, 83.85.Hf, 61.20.-p

I. INTRODUCTION AND MOTIVATION

In aqueous solutions, amphiphiles show very rich and interesting behaviour governed by the tendency of the molecules to self-organise into structures where the hydrophobic regions of molecules tend to be pushed together and away from the water, enabling the hydrophilic headgroups to hydrogen-bond more easily to the surrounding water molecules. This results in various supramolecular assemblies including micelles, columnar phases and lamellar structures depending on concentration and temperature. An emerging route toward the development, testing and refinement of detailed molecular models of the hydrophobic interaction, hydration and the physics of aqueous macromolecules involves the use of small molecule systems (such as lower alcohols) as "prototypes".

Despite their structural simplicity, it is well known that the thermodynamic and transport properties of alcohol-water mixtures, such as the mean molar volume, the diffusion coefficient, the compressibility and the excess entropy, are significantly smaller, and the viscosity significantly larger, than the values that might be expected from an ideal mixture of the pure liquids [1, 2, 3, 4, 5, 6]. The longstanding explanation of these effects in terms of an enhanced structuring of the water in the presence of the alcohol [7] does not appear to be supported by modern diffraction experiments [8, 9, 10, 11] and an alternative model is needed. Recent neutron diffraction studies of alcohol-water binary mixtures [8, 9, 12, 13] are leading to new insights into the behaviour of water near molecules containing both hydrophobic and hydrophilic groups. These have established that, in the dilute alcohol limit, the alcohol molecule appears to have a mild compressive effect on the water structure, as is seen from the slight inward movement of the second peak of the water-

oxygen radial distribution function compared to the same function in pure water. This second peak, which occurs near $r = 4.5$ Å in the $O_W O_W$ radial distribution function of pure water, has widely been interpreted as the signature of the tetrahedral ordering in water. By contrast, in the opposite (concentrated alcohol) limit, the system segregates into what is effectively a molecular-scale microemulsion [8], with methyl head groups pushed towards each other, and the hydrophilic hydroxyl groups forming a boundary around small pockets of a water-like fluid.

These simple systems have also been the subject of considerable computational investigations. The earliest of these [14, 15, 16] used Monte Carlo methodologies at low or infinitely dilute concentrations of alcohol. Despite different computational models, and some apparent contradictions between their results, they all found an enhanced cage-like structure of water around the methyl group, in accordance with the Frank and Evans model [7]. Later, MD simulations explored other mixture compositions [17, 18] using effective potential models. Tanaka and Gubbins [19] were amongst the first to highlight the role of the water-water interactions in discussing aqueous solutions. More recently, Meng and Kollman [20] have performed MD simulations of various solutes (including methanol) at infinite dilution and found that the water structure around the hydrophobic groups is preserved rather than enhanced. Laaksonen et al [21] have explored several concentrations though there was no specific attention given to clustering. Ab initio simulations of alcohol-water mixtures have also recently been reported [22, 23], however the computational expense of these simulations is such that they are restricted to picosecond simulation on small system sizes. Nonetheless, these studies have also pointed to the lack of structural enhancement of the water surrounding the hydrophobic moiety in the alco-

hol. Very recently, some of us have obtained preliminary results from MD simulations of an alcohol-rich methanol-water solution that does exhibit extreme clustering and micro-inmiscibility [24].

Given the ongoing interest in these systems [25, 26], the availability of experimental data only at dilute and concentrated alcohol limits, and the apparently contradictory results from computer simulation there is a strong motivation to undertake a systematic survey of extended structure (clustering) as a function of concentration in the model aqueous methanol system using both experimental and simulation techniques performed at identical state points. We are specially interested in exploring the changes in the clustering behaviour as a function of concentration, and the extent to which molecular dynamics simulations account for the experimental observations and can provide additional insight into clustering dynamics.

II. EXPERIMENTAL METHODS

A. Neutron diffraction experiments

Protiated and deuteriated samples of methanol and water were obtained from Sigma-Aldrich and used without additional purification. Neutron diffraction measurements were performed on the SANDALS time-of-flight diffractometer on the ISIS pulsed neutron source at the Rutherford Appleton Laboratory, U.K. Samples were placed in flat plate cells made from a Ti-Zr alloy that gives negligible coherent scattering. These were mounted on a closed cycle refrigerator, and neutron diffraction measurements were made at temperatures of 293K (with mole fraction $x = 0.05$, $x = 0.27$, $x = 0.7$) and 298K ($x = 0.54$) respectively. Corrections for attenuation and multiple scattering were made using the ATLAS program suite. A further correction for inelastic scattering was also made [27]. The differential scattering cross-section for each sample was obtained by normalising to a vanadium standard sample. A total of 7 samples were measured – see Figure 1 for $x = 0.54$. These were respectively (i) CD_3OD in D_2O ; (ii) CD_3OH in H_2O ; (iii) a 50:50 mixture of (i) and (ii); (iv) CH_3OD in D_2O ; (v) a 50:50 mixture of (i) and (iv); (vi) CH_3OH in H_2O ; and (vii) a 50:50 mixture of (i) and (vi). For $x = 0.055$ samples were measured (i), (ii), (iii), (vi) and (vii). These procedures lead to a structure factor $F(Q)$ having the form $F(S_{HH}(Q); S_{XH}(Q); S_{XX}(Q))$ where $S_{HH}(Q)$ gives correlations between labelled atoms and $S_{XH}(Q)$ and $S_{XX}(Q)$ are the two composite partial structure factors which give the remaining correlations between other types of atoms (X) and the labelled atom type (H) in the form of a weighted sum of individual site-site partial structure factors.

B. Empirical potential structure refinement

A mixture of methanol and water contains 6 distinct atomic components, namely C, O, M and H on the methanol molecule (here M represents the methyl hydrogen atom while H represents the hydroxyl hydrogen atom), and O_w and H_w on the water molecule. A full structural characterisation of the system therefore requires the determination of 21 site-site radial distribution functions, which is well beyond the possibility of any existing diffraction techniques by themselves.

Therefore to build a model of the liquid structure, the experimental data are used to constrain a computer simulation of the mixture. However, unlike conventional simulations the empirical potential used here is obtained directly from the diffraction data and has the effect of driving the structure of the three-dimensional model solution toward configurations that are consistent with the measured partial structure factors [28]. A total of 600 molecules (methanol and water) are contained in a cubic box of the appropriate dimension to give the measured density of each solution at the appropriate temperature (see Table I). Periodic boundary conditions are imposed. Reference interatomic potentials for water and methanol are taken from the literature [29]. A comparison between the experimentally-measured partial structure factors and those generated from the ensemble-averaged EPSR configurations is shown in Figure 1.

In the present case a single set of site-site empirical potential coefficients was refined against the methanol-water data at each concentration, as well as for pure water [31] and for pure methanol [32]. The result is a set of site-site empirical potentials which are consistent with methanol-water solutions over the full range of concentrations. Comparing the results of these simulations with those where the empirical potential coefficients are refined separately for each concentration revealed some discrepancies in the detail of the extracted $\text{O}_w - \text{O}_w$ radial distribution function, particularly at the higher methanol concentrations. Clearly the diffraction data by themselves do not constrain this function sufficiently to give a completely unambiguous $\text{O}_w - \text{O}_w$ radial distribution function. These discrepancies however do not affect the main conclusions of this paper, which are to do with the way methanol and water form distinct local clusters when mixed. We hope to present a more exhaustive study of the uncertainties involved in the EPSR analysis of molecular liquids and mixtures in a separate publication.

III. SIMULATION AND CLUSTER ANALYSIS METHODS

We have performed classical molecular dynamics simulations within the NVT ensemble, utilising previously tested intermolecular potentials for both methanol [33] and water [34] that have been shown to predict the struc-

Mole fraction x	Temp. /K	Total No. molecules	No. of methanol molecules	No. of water molecules	No. density / atom s/A ³	Size /Å/K	Total No. molecules	No. methanol molecules	No. water molecules	No. density / atom s/A ³	B
0.05	293	600	30	570	0.0927	26.898	600	162	438	0.0968	
0.27	293	600	162	438	0.0953	28.898	600	324	276	0.0953	
0.54	298	600	324	276	0.0950	30.298	424	297	127	0.0934	
0.70	293	600	420	180	0.0930	32.04					

TABLE I: Parameters of the methanol-water mixtures used in the Empirical Potential Structural Re-nement

ture and dynamics of the single component liquids well. Both molecules are modelled as fully flexible entities, with explicit potential terms for each type of atom center. Using the DL-POLY code [35], we have performed simulations of 2ns duration with a timestep of 0.5fs on systems of $x=0.27$, $x=0.54$ and $x=0.7$ mole fraction. The parameters relevant to these simulations are given in Table II. All simulations were equilibrated for 0.5ns prior to data collection and trajectory snapshots were saved every 0.1ps for subsequent analysis.

In analysing both the experimentally-constrained EP SR configurations and molecular dynamics trajectories, an identical definition of a cluster is made based on bond connectivity. Specifically, water molecules are assigned to the same cluster if they can be connected by a continuous hydrogen-bond network. The criterion used is that two water molecules are said to be hydrogen-bonded if their constituent oxygen atoms are less than $R_{O_W O_W}$ apart, where $R_{O_W O_W}$ is determined as the minimum following the first peak in the $O_W O_W$ pair correlation function (approximately 3.5Å for both simulated and EP SR-fitted functions). For the methanol molecules, clusters may be defined in one of two ways. When investigating hydrogen-bonded clusters, we use the same criterion as for water, i.e. if constituent methanol oxygen atoms are less than R_{O_O} apart. However we also investigate clustering of methanol molecules via methyl group association. In this case, two methanol molecules are assigned to the same cluster if the C-C distance is less than the minimum following the first peak determined from the CC pair correlation function (which is approximately 5.7 Å). According to this criterion, methanol molecules that are in contact only via their nonpolar groups are not within the same (hydrogen-bonded) cluster.

When plotting cluster distribution histograms, we plot the number of clusters of a size i , $m(i)$, as a fraction of the total number of clusters, M , where $M = \sum_i m(i)$. Cluster lifetimes were deduced from the MD trajectories by calculating the average duration that a cluster persists with at least one participant member from the previous trajectory snapshot. The distinction is made between clusters of size 1 (i.e. with no H-bonded neighbours) and those of larger sizes.

We have investigated the dependence of cluster distributions obtained on the size of the system employed. Using four different system sizes ranging from 700 to nearly 18000 particles, we find that the cluster distributions and

TABLE II: Parameters of the methanol-water mixtures used in the Molecular Dynamics Simulations

lifetimes are practically identical in all cases and conclude that our observations are not significantly dependent on the choice of system size.

IV. RESULTS AND DISCUSSION

A. Local structure

A comparison of radial distribution functions $g(r)$ for CC and $O_W O_W$ is shown in Fig 2. A concentration of $x = 0.27$ and the pure solvents (water $x = 0.0$ and methanol $x = 1.0$) are shown for both the experimentally-constrained EP SR configurations and the molecular dynamics simulations. Local structure therefore appears similar in both the experimental and computational results. There are subtle differences between the experiment and simulation particularly the $g(r)$ for CC which could be due to different potentials used in the fitting procedure and the different treatments of methyl group flexibility. However, it is clear that there is good qualitative agreement when we go on to explore extended structures in the solutions.

B. Clustering and cluster lifetime

We consider first the results of the neutron diffraction experiments. Visual inspection of the boxes of atoms reveals significant segregation of water from methanol at all concentrations. An example is shown for $x = 0.54$ in Fig 3. Visual inspection also suggests that the methanol clusters do not tend to form hydrogen-bonded chains to the same extent as in the pure alcohol. Instead the methyl headgroups tend to be in contact, with the hydroxyl headgroups bonding to water molecules forming the main boundary between methanol- and water-rich regions. This is broadly as expected for a hydrophobically-driven system and is what has been observed in earlier diffraction work [12, 13]. Similar snapshots are obtained from the molecular dynamics simulations (not shown).

Further evidence of the way in which the presence of water affects the structure and orientation of methanol molecules is obtained from investigation of the size of hydrogen-bonded methanol clusters from the MD simulations and radial distribution functions. Compared to the hydrogen-bonded network in the pure liquid, the cluster sizes are much smaller. For example, in

the methanol-rich solution ($x=0.7$) we find about 75 % of the hydrogen-bonded methanol clusters consist of only 1,2 or 3 methanol molecules. For comparison, in pure methanol the fraction of clusters of the same size range drops to around 37 %, with the majority of hydrogen-bonded clusters containing more than 3 methanol molecules[24]. This indicates a substantial disruption to the methanol hydrogen-bonded network. The orientation of the methanol molecules is also affected; in the solution the methyl headgroups are pushed closer together, as evidenced by a shift to smaller r values of the first peaks in g_C and g_{MM} , where M denotes a methyl hydrogen, in both the EPSR procedure and MD simulations.

The persistence of clustered structures in these systems is reflected in the average lifetime of clusters and single molecules. An estimate of these lifetimes can be obtained from analysis of the molecular dynamics trajectories and are particularly interesting in the simulation performed at the $x = 0.7$ methanol mole fraction. Firstly, we observe that individual water molecules are short-lived and survive, on average, for only 2 ps before being absorbed into a cluster. However, in rare cases, lifetimes of 100 ps are found. A similar result is found for the other cluster sizes which show average lifetimes of about 3ps though there are also persistent clusters surviving for up to 0.5 ns. The methanol hydrogen-bonded clusters, already noted to be much reduced in size by the presence of the water, are extremely short-lived; most persist for approximately 1ps with no methanol hydrogen-bonded structure lasting for more than 40ps. Thus the simulation results, in addition to being consistent with the overall structures implied by the neutron diffraction data, also suggest that the extended structures characterising the methanol-water system are very dynamic with rapid shedding and reforming of cluster members.

C . Percolation

We now explore clustering of both species quantitatively as a function of concentration where an identical definition of a cluster is made in analysing both the experimentally-constrained EPSR configurations and molecular dynamics trajectories. For water molecules the hydrogen-bond definition was used to designate which molecules belong to a given water cluster, while for methanol clusters the C-C distance definition was used, as this criterion is more indicative of the nature of the methanol clustering than the hydrogen bond criterion.

The cluster size distributions as obtained from the EPSR ensembles (for $x = 0.7; 0.54; 0.27$ and 0.05) and molecular dynamics simulation (for $x = 0.7; 0.54$ and 0.27) are shown in Fig 4 along with the predicted power law $n_s \propto s^{-2.2}$ for random percolation on a 3-d cubic lattice[36]. The experimental and computational results both give similar results for the cluster size distribution at the three concentrations for which a

direct comparison can be made as was implied by visual inspection of the EPSR and molecular dynamics structures.

Several "special" concentrations emerge as defined by changes in clustering behaviour. Specifically, $x = 0.27$ determines the approximate alcohol concentration below which water percolates throughout the mixture while methanol does not – occurring instead only in small, isolated clusters. Above this molar fraction, however, methanol percolates throughout the mixture. The larger water clusters also percolate (at $x = 0.54$, see Fig.4) but become increasingly isolated until they are confined to distinct, non-spanning clusters by $x = 0.7$. Thus, according both to the experimentally-constrained EPSR data and the MD simulations, in the approximate concentration range defined by $0.27 < x < 0.54$ both water and alcohol clusters percolate simultaneously, making this a bi-percolating liquid mixture.

Significantly, the mole fraction range over which simultaneous two-component percolation occurs coincides closely with the concentration at which many thermodynamic properties show extrema[37, 38, 39, 40, 41, 42]. This suggests that the nature and extent of clustering in these mixtures may offer a structural explanation for the thermodynamic anomalies.

In earlier work on liquids, computer simulations have identified percolation transitions in supercritical Lennard-Jones fluids[43], supercritical water[44], water in aqueous acetonitrile[45] and aqueous tetrahydrofuran (THF) [46, 47]. However, to our knowledge this is the first report of simultaneous percolation of two fully miscible fluids. Despite subtle variation in the cluster size distribution, we have obtained independent evidence of two-component percolation from experimental and computational methods.

D . Dimensionality of clusters

A further feature of the EPSR clusters is revealed in Fig 5 which shows the typical surface area per molecule. We now explore clustering of both species quantitatively as a function of concentration where an identical definition of a cluster is made in analysing both the experimentally-constrained EPSR configurations and molecular dynamics trajectories. For water molecules the hydrogen-bond definition was used to designate which molecules belong to a given water cluster, while for methanol clusters the C-C distance definition was used, as this criterion is more indicative of the nature of the methanol clustering than the hydrogen bond criterion.

The cluster size distributions as obtained from the EPSR ensembles (for $x = 0.7; 0.54; 0.27$ and 0.05) and molecular dynamics simulation (for $x = 0.7; 0.54$ and 0.27) are shown in Fig 4 along with the predicted power law $n_s \propto s^{-2.2}$ for random percolation on a 3-d cubic lattice[36]. The experimental and computational results both give similar results for the cluster

size distribution at the three concentrations for which a direct comparison can be made as was implied by visual inspection of the EPSR and molecular dynamics structures.

Several "special" concentrations emerge as defined by changes in clustering behaviour. Specifically, $x = 0.27$ determines the approximate alcohol concentration below which water percolates throughout the mixture while methanol does not – occurring instead only in small, isolated clusters. Above this molar fraction, however, methanol percolates throughout the mixture. The larger water clusters also percolate (at $x = 0.54$, see Fig. 4) but become increasingly isolated until they are confined to distinct, non-spanning clusters by $x = 0.7$. Thus, according both to the experimentally-constrained EPSR data and the MD simulations, in the approximate concentration range defined by $0.27 < x < 0.54$ both water and alcohol clusters percolate simultaneously, making this a bi-percolating liquid mixture.

Significantly, the mole fraction range over which simultaneous two-component percolation occurs coincides closely with the concentration at which many thermodynamic properties show extrema [37, 38, 39, 40, 41, 42]. This suggests that the nature and extent of clustering in these mixtures may offer a structural explanation for the thermodynamic anomalies.

In earlier work on liquids, computer simulations have identified percolation transitions in supercritical Lennard-Jones fluids [43], supercritical water [44], water in aqueous acetonitrile [45] and aqueous tetrahydrofuran (THF) [46, 47]. However, to our knowledge this is the first report of simultaneous percolation of two fully miscible fluids. Despite subtle variation in the cluster size distribution, we have obtained independent evidence of two-component percolation from experimental and computational methods. The area to volume ratio (as represented by the number of water molecules in a cluster which form hydrogen bonds with a methanol molecule divided by the number of water molecules in the cluster) for water molecules prior to the percolation transition, together with an exactly analogous quantity for the methanol clusters. Clearly the ratio does not decay as $N^{-1/3}$ as would be expected for a 3-dimensional object: the clusters appear to maximise their surface area by forming as many bonds as possible with methanol. The observed behaviour corresponds much more closely to a 2-dimensional object, suggesting the clusters occur in the form of disordered sheets or cylinders, rather than the sphere-like objects that might be expected in conventional micelle formation. Only at the highest water content, $x = 0.05$, do the water clusters appear to have adopted 3D characteristics.

This broad conclusion is also supported by the analysis of the topologies of the water clusters predicted from the MD simulations. Figure 6 shows the variation of the average radius of gyration of all the clusters of size i ($R(i)$) as a function of cluster size, for three different solution

compositions. The cluster topology can be characterised by a fractal dimension d , determined by a power law fit to the data in Figure 6, such that $R(i) \propto i^{d/3}$. For solutions of methanol mole fractions of $x = 0.7, 0.54$ and 0.3 , these values of d are determined to be $1.69, 1.89$ and 2.03 , respectively. We note that as the mole fraction of water (and hence the proportion and size of larger clusters) increases the characteristic dimension increases. Interestingly, the cluster topologies of small clusters determined from our simulations are insensitive to changes in composition; all three compositions exhibit similar fractal dimension ($d \approx 1.6$) for clusters sizes up to $i = 20$. These results indicating the 2-d fractal dimension of water clusters over a range of compositions is in agreement with the results of a simulation study by Oleinikova et al [46] on the percolation of water clusters in the vicinity of a region of immiscibility in an aqueous solution of THF. Simultaneous bi-percolation of both THF and water was found in this study, with THF percolating clusters having a characteristic fractal dimension of 2.5 and those of water approximately 1.9 . Visual inspection of some of our percolating clusters (of both methanol and water) reveal that these clusters span all six faces of the simulation box.

V. SUMMARY AND CONCLUSION

Isotope-labelled neutron diffraction measurements analysed using the empirical potential structural refinement method have been combined and compared with independent molecular dynamics simulations at identical state points to explore structure in methanol-water mixtures at several concentrations. We find that local and extended structures are well described by both methods and lead to similar conclusions. We find highly heterogeneous mixing across the entire concentration range despite apparent miscibility of both components in all proportions. Extended chain, sheet and three-dimensional structures form depending on concentration.

At a particular concentration regime near $x = 0.27$ these structures form percolating networks for both components. This concentration has long been considered "special" as it is near the point where many transport coefficients and thermodynamic functions have extremal values. Other alcohols also show extrema of these same material properties (at lower mole fractions) and the present work suggests a structural basis for these observations connected to the details of mixing heterogeneities.

Acknowledgements

We are grateful to I. Brovchenko and G. Martyna for very helpful discussions

-
- [1] R. Gibson, *J. Chem. Phys.* 57, 1551 (1935).
- [2] R. Lama and B. C.-Y. Lu, *J. Chem. Eng. Data* 10, 216 (1965).
- [3] H. Schott, *J. Chem. Eng. Data* 14, 236 (1969).
- [4] T. Yergovich, G. Swift, and F. Kurata, *J. Chem. Eng. Data* 16, 222 (1971).
- [5] M. McGlashan and A. Williamson, *J. Chem. Eng. Data* 21, 196 (1976).
- [6] S. Randzio and I. Tomaszewicz, *Thermochimica Acta* 103, 281 (1986).
- [7] H. Frank and M. Evans, *J. Chem. Phys.* 13, 507 (1945).
- [8] S. Dixit, J. Crain, W. Poon, J. Finney, and A. Soper, *Nature* 416, 829 (2002).
- [9] S. Dixit, A. Soper, J. Finney, and J. Crain, *Europhys. Lett.* 59, 377 (2002).
- [10] J. Finney and A. Soper, *Phys. Rev. Lett.* 71, 4346 (1993).
- [11] J. L. Finney, D. T. Bowron, R. M. Daniel, P. A. Timmins, and M. A. Roberts, *Biophys. Chem.* 105, 391 (2003).
- [12] D. Bowron, A. K. Soper, and J. L. Finney, *J. Chem. Phys.* 114, 6203 (2001).
- [13] D. Bowron, J. L. Finney, and A. K. Soper, *J. Phys. Chem. B* 102, 3551 (1998).
- [14] G. Bolis, C. Corongui, and E. Clementi, *Chem. Phys. Lett.* 86, 299 (1982).
- [15] W. Jorgensen and J. Madura, *J. Am. Chem. Soc.* 105, 1407 (1983).
- [16] S. Okazaki, H. Touhara, and K. Nakanishi, *J. Chem. Phys.* 81, 890 (1984).
- [17] G. Palinkas, E. Hawlicka, and K. Heinzinger, *Chem. Phys.* 158, 65 (1991).
- [18] M. Ferrario, M. Haughney, I. McDonald, and M. Klein, *J. Chem. Phys.* 93, 5156 (1990).
- [19] H. Tanaka and K. Gubbins, *J. Chem. Phys.* 97, 2626 (1992).
- [20] E. Meng and P. Kolman, *J. Phys. Chem.* 100, 11460 (1996).
- [21] A. Laaksonen, P. Kusalik, and I. Svishchev, *J. Phys. Chem. A* 101, 5910 (1997).
- [22] T. van Erp and E. Meijer, *J. Chem. Phys.* 118, 8831 (2003).
- [23] J.-W. Handgraaf, T. van Erp, and E. Meijer, *Chem. Phys. Lett.* 367, 617 (2003).
- [24] S. Allison, R. Hargreaves, J. Fox, and S. Bates, *Phys. Rev. Lett.* submitted (2004).
- [25] T. Sato, A. Chiba, and R. Nozaki, *J. Chem. Phys.* 112, 2924 (2000).
- [26] Y. Koga, *J. Phys. Chem.* 100, 5172 (1996).
- [27] A. K. Soper and A. Luzar, *J. Chem. Phys.* 97, 1320 (1992).
- [28] A. Soper, *Chem. Phys.* 202, 295 (1996).
- [29] M. Haughney, M. Ferrario, and I. R. McDonald, *J. Phys. Chem.* 91, 4934 (1987).
- [30] H. J. C. Berendsen, J. R. Grigera, and T. P. Straatsma, *J. Phys. Chem.* 91, 6269 (1987).
- [31] A. K. Soper, *J. Chem. Phys.* 258, 121 (2000).
- [32] T. Yamaguchi, K. Hidaka, and A. K. Soper, *Mol. Phys.* 96, 1159 (1999).
- [33] J. Pereira, C. Catlow, and G. Price, *J. Phys. Chem. A* 105, 1909 (2001).
- [34] M. Levitt, M. Hirschberg, R. Sharon, K. Laidig, and V. Daggett, *J. Phys. Chem. B* 101, 5051 (1997).
- [35] W. Smith and T. Forester, *J. Mol. Graphics* 14, 136 (1996).
- [36] N. Jan, *Physica A* 266, 72 (1999).
- [37] R. E. Gibson, *J. Am. Chem. Soc.* 57, 1551 (1935).
- [38] R. F. Lama and B. C.-Y. Lu, *J. Chem. Eng. Data* 10, 216 (1965).
- [39] I. Tomaszewicz, S. L. Randzio, and P. Gierczy, *Thermochimica Acta* 103, 281 (1986).
- [40] H. Schott, *J. Chem. Eng. Data* 14, 237 (1965).
- [41] Z. J. Derlacki, A. J. Eastale, A. V. J. Edge, L. A. Woolf, and Z. Roksandic, *J. Phys. Chem.* 89, 5318 (1985).
- [42] K. Soliman and E. Marschall, *J. Chem. Eng. Data* 35, 375 (1990).
- [43] N. Yoshii and S. Okazaki, *J. Chem. Phys.* 107, 2020 (1997).
- [44] A. Kalinichev and S. Churakov, *Fluid Phase Equilibria* 183-184, 271 (2001).
- [45] D. Bergman and A. Laaksonen, *Phys. Rev. E* 58, 4706 (1998).
- [46] A. Oleinikova, I. Brovchenko, A. Geiger, and B. Guillot, *J. Chem. Phys.* 117, 3296 (2002).
- [47] I. Brovchenko, A. Geiger, and A. Oleinikova, *Phys. Chem. Chem. Phys.* 6, 1982 (2004).

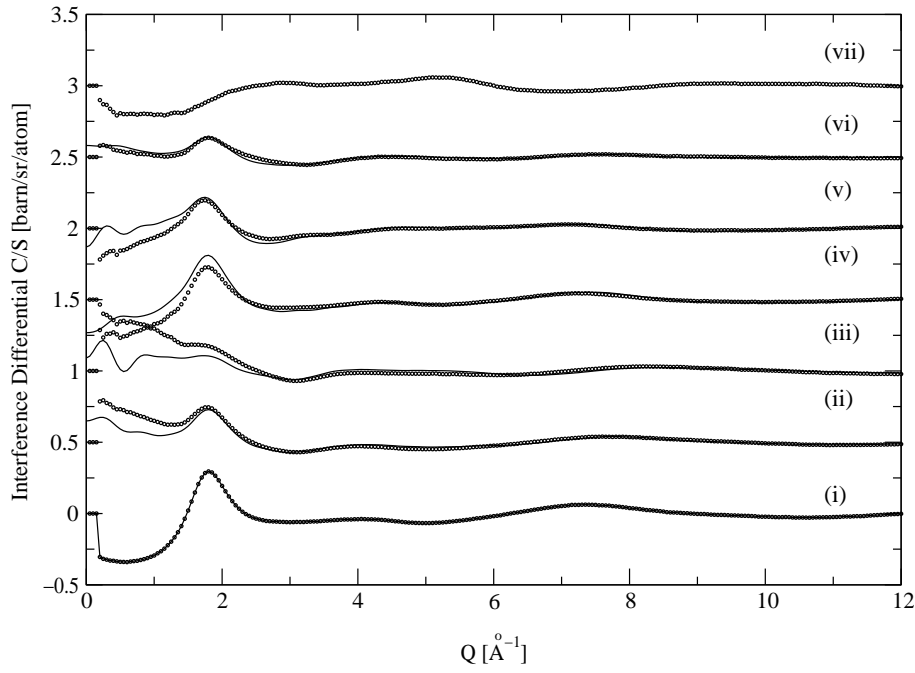


FIG. 1: Typical example of the fits (lines) obtained by the EPSR computer simulation procedure compared to the original data (circles). The data shown in this case ($x = 0.54$) are the interference differential scattering cross-sections for the samples (i) through (vii) described under Methods. Discrepancies are observed in the low Q region. These are caused by difficulties in removing completely the effect of nuclear recoil from the measured data. However this recoil effect is expected to have only a monotonic dependence on Q and so is unlikely to influence the model structure to any significant extent.

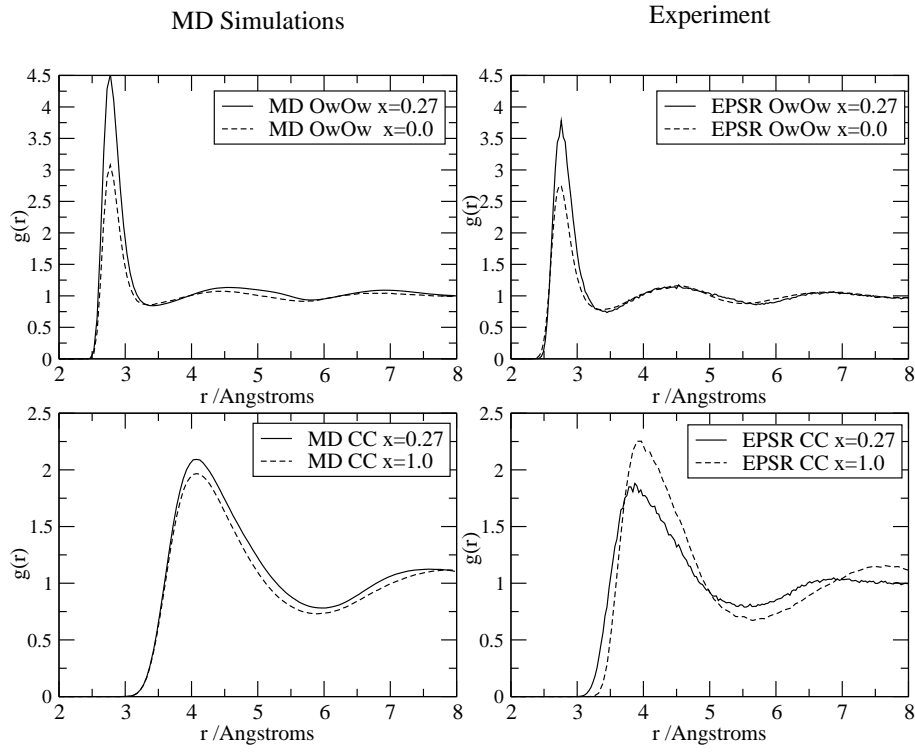


FIG. 2: Comparison of the radial distribution function $g(r)$ as obtained from molecular dynamics (MD) time averages (left) and experimentally-constrained EPSR ensemble averages (right). The data shown is for the $x = 0.27$ mixture in relation to the pure solvents, water ($x = 0.0$) and methanol ($x = 1.0$), for both the O_w-O_w (top) and the $C-C$ radial distribution functions (bottom).

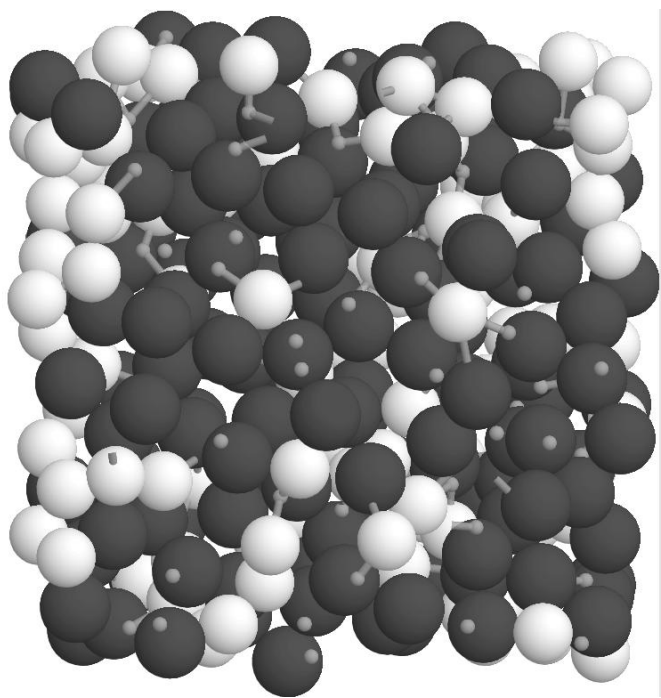


FIG. 3: Snapshot of an experimentally-constrained EPSR model of the methanol-water mixture at $x = 0.54$ showing clusters of the segregated components. Methyl groups are shown as black spheres, large white spheres highlight the position of water molecules and small grey spheres denote methanol oxygen atoms.

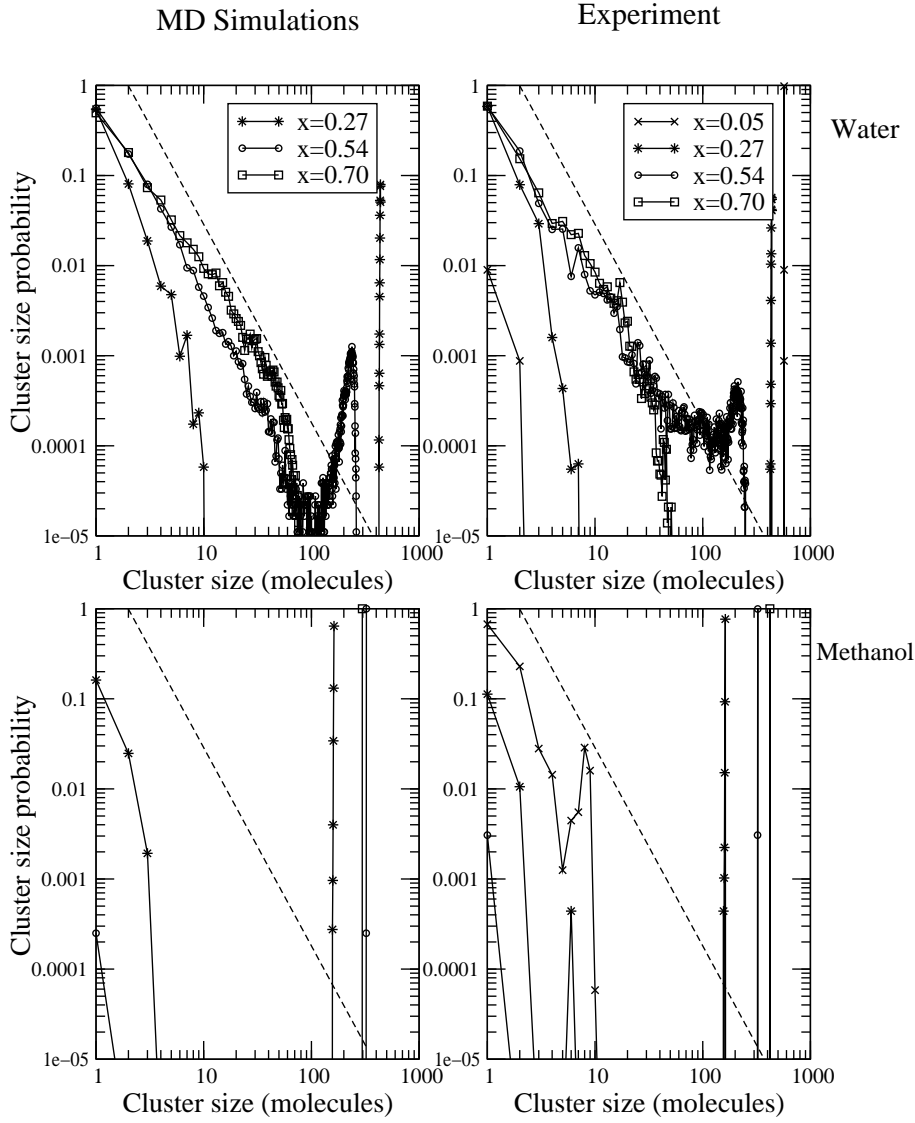


FIG. 4: Cluster size distributions for water(top) and methanol(bottom) clusters in methanol-water mixtures. For water molecules the hydrogen-bond definition was used to designate which molecules belong to a given water cluster, while for methanol clusters the C-C distance definition was used. On the left, from MD simulations with methanol mole fractions 0.27, 0.54 and 0.7 and on the right from neutron diffraction experiments for methanol mole fractions 0.05, 0.27, 0.54 and 0.7. The dashed lines show the predicted cluster size distribution at the percolation threshold [36]. Percolation in the simulated box occurs when clusters of a size close to the number of molecules in the simulation box form (vertical lines on the right hand side of the plot).

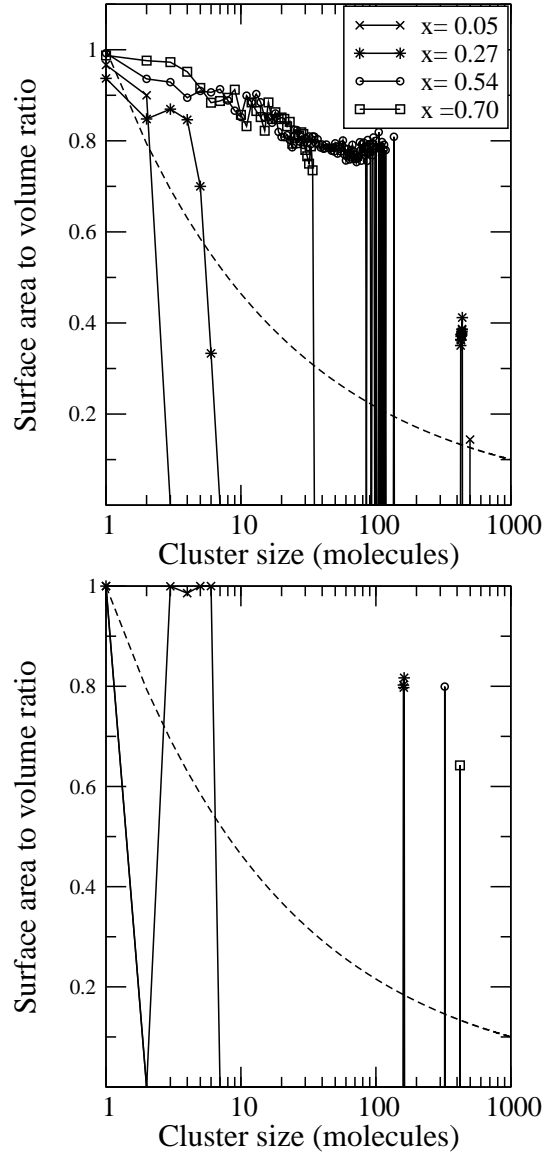


FIG. 5: Ratio of number of water molecules at the surface of a cluster (as defined by being hydrogen bonded to a methanol hydroxyl group) to total number of water molecules in a cluster (top). The dashed line shows the $N^{-1/3}$ behaviour that would be expected for this ratio if the clusters grew equally in 3 dimensions with N the number of molecules in a cluster. Only for the fully percolating water cluster at $x = 0.05$ do the clusters show normal 3D behaviour. Ratio of number of methanol molecules at the surface of a cluster to total number of methanol molecules in a cluster (below). Here even at $x = 0.7$ the methanol clusters do not approach full 3D behaviour.

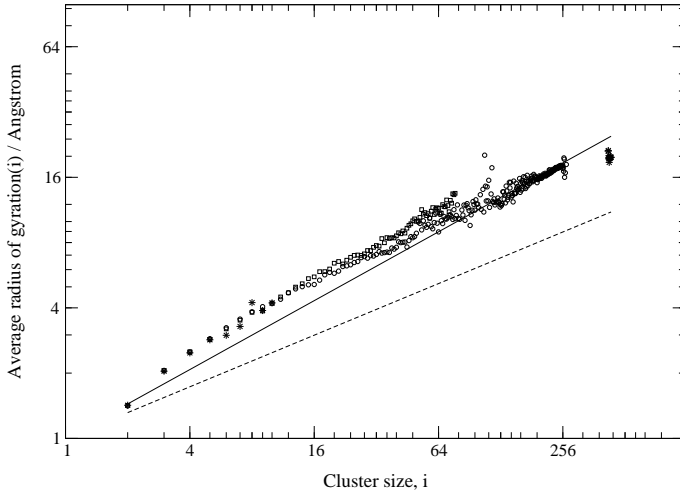


FIG. 6: Average radius of gyration of all water clusters of size i as a function of cluster size i , in solutions of different composition from MD simulations. The composition of the solutions, in terms of mole fractions of methanol, are $x=0.7$ (squares), 0.54 (circles), 0.3 (stars). The solid and dashed lines represent the variation of average radius of gyration with cluster size of percolating clusters on 2-d square lattice (characterised by $d=91/48$) and 3-d cubic lattice (characterised by $d=2.53$), respectively, as determined from large lattice random site percolation simulations[36].